Available online at www.sciencedirect.com
ScienceDirect
Journal of Nuclear Materials 375 (2008) 370–381
journal of nuclear materials
www.elsevier.com/locate/jnucmat

The influence of neutron irradiation in FFTF on the microstructural and microchemical development of Mo–41Re at 470–730 °C

D.J. Edwards, F.A. Garner *, D.S. Gelles

Pacific Northwest National Laboratory, Richland, WA, USA

Received 15 November 2007; accepted 17 January 2008

Abstract

Specimens of Mo–41 wt% Re irradiated in the fast flux test facility (FFTF) experience significant and non-monotonic changes in density that arise first from radiation-induced segregation, leading to non-equilibrium phase separation, and second by progressive transmutation of Re to Os. As a consequence the density of Mo–41Re initially decreases and then increases thereafter. Beginning as a single-phase solid solution of Re and Mo, irradiation of Mo–41 wt% Re over a range of temperatures (470–730 °C) to 28–96 dpa produces a high density of thin platelets of a hexagonal close-packed (hcp) phase identified as a solid solution of Re, Os and possibly a small amount of Mo. These hcp precipitates are thought to form in the alloy matrix as a consequence of strong radiation-induced segregation to Frank loops. Grain boundaries also segregate Re to form the hcp phase, but the precipitates are much bigger and more equiaxed in shape. Although not formed at lower dose, continued irradiation at 730 °C leads to the co-formation of late-forming chi-phase, an equilibrium phase that then competes with the preexisting hcp phase for rhenium.

1. Introduction

The search for materials to serve as structural components of proposed nuclear energy or spacecraft devices has led to the exploratory irradiation of a wide variety of metals and alloys. Molybdenum and its alloys, including those of the Mo–Re system, have been proposed as potential candidates for such service because of their inherently high melting point and strength, room temperature fabricability, and an acceptable match with the coefficients of thermal expansion for carbon and tungsten in fusion first wall applications.

There have been a number of studies [1–23] on the Mo–Re system and its behavior after neutron or charged particle irradiation, but insufficient data have been published on the microstructural and transmutation-induced microchemical evolution that causes degradation of physical and mechanical properties, especially at high neutron exposures, high temperatures and very high Re levels. Only a few of the above-referenced studies examined the post-irradiation microstructure.

Singh and coworkers [11,12] investigated the microstructure and mechanical properties of Mo–5%Re irradiated in the DR-3 reactor to ~0.16 dpa at temperatures of 50–450 °C and observed only dislocation loops. There were no precipitates or voids under these conditions. Chakin and coworkers [13] also investigated Mo–Re alloys at 15%, 20%, 30%, and 41% Re irradiated in the SM-2 reactor to relatively low neutron exposures at temperatures of 120–160 °C. They also did not observe any precipitates, but only dislocation loops.

Hasegawa et al. [14] investigated Mo–5 wt% Re irradiated in the FFTF fast reactor at five temperatures ranging from 373 to 800 °C and dose levels of 7–34 dpa. They observed small voids under all irradiation conditions studied but precipitates were formed only in specimens irradiated above 520 °C. They also observed plate-like

* Corresponding author. Tel.: +1 509 376 4136; fax: +1 509 376 0418.
E-mail address: frank.garner@pnl.gov (F.A. Garner).

0022-3115/$ - see front matter © 2008 Elsevier B.V. All rights reserved.
doi:10.1016/j.jnucmat.2008.01.014

precipitates but they did not identify their crystal structure or composition.

In a later paper involving Mo–5Re and Mo–41Re (wt%) from the same irradiation series, Hasegawa and coworkers showed that increasing the Re content from 5% to 41% led to a suppression of void formation at 41 wt% Re in FFTF for doses ranging from 7 to 34 dpa depending on irradiation temperature, but the precipitation became much more pronounced and complicated [16]. There were (1) relatively large needle or thin plate precipitates at 373 °C, (2) fine needle or rectangular type precipitates at 406, 519 and 600 °C, and (3) large blocky and plate type precipitates at 800 °C. The precipitates were not identified in this study, but it was noted by Hasegawa that Garner and coworkers [20] had previously identified the plate-type precipitates as being a Re-rich hcp phase at 645 and 730 °C.

Nemoto and coworkers [17] extended the studies of Hasagawa, irradiating Mo–Re alloys at 2, 4, 5, 10, 13, and 41 wt% Re, concluding that at ~20 dpa in FFTF sigma phase and chi-phase precipitates were formed in all specimens irradiated in the range 406–800 °C, regardless of whether the Re content was low (2, 4, 5, 10, and 13 wt%) or high at 41 wt%. However, their conclusion was based primarily on comparisons with more extensive microscopy in a similar parallel study in FFTF conducted on W–26 wt% Re [19]. Nemoto and coworkers did not identify the hcp phase in Mo–41Re that was observed by Garner and coworkers at somewhat higher doses [20], however. This difference in conclusion produces some uncertainty concerning the identity of the precipitate phases forming in Mo–Re at the 41 wt% Re level. Addressing this uncertainty is the primary focus of this paper.

The identification of chi-phase precipitates in relatively dilute Mo–5Re by Nemoto is noteworthy since the equilibrium phase diagram shown in Fig. 1 predicts that only a solid solution should exist at that composition and temperature range [24]. Therefore a very strong radiation-driven mechanism to produce segregation is required to reach the 86–88 wt% Re levels characteristic of chi-phase in the unirradiated condition. Although somewhat less segregation is need to produce sigma phase (~65–80%) it is also surprising that Nemoto observed sigma phase in his irradiation series since the phase diagram in Fig. 1 would predict that sigma would form only above 1125 °C.

In Mo–Re alloys containing Re at 13, 42 and 45 wt%, radiation-induced segregation and precipitation have been observed by Erck and Rehn [21–23]. Their ion irradiation experiments yielded high concentrations of Re at or near the foil surfaces and grain boundaries, and produced chi-phase precipitates in >40 wt% Re specimens irradiated at temperatures greater than 750 °C.

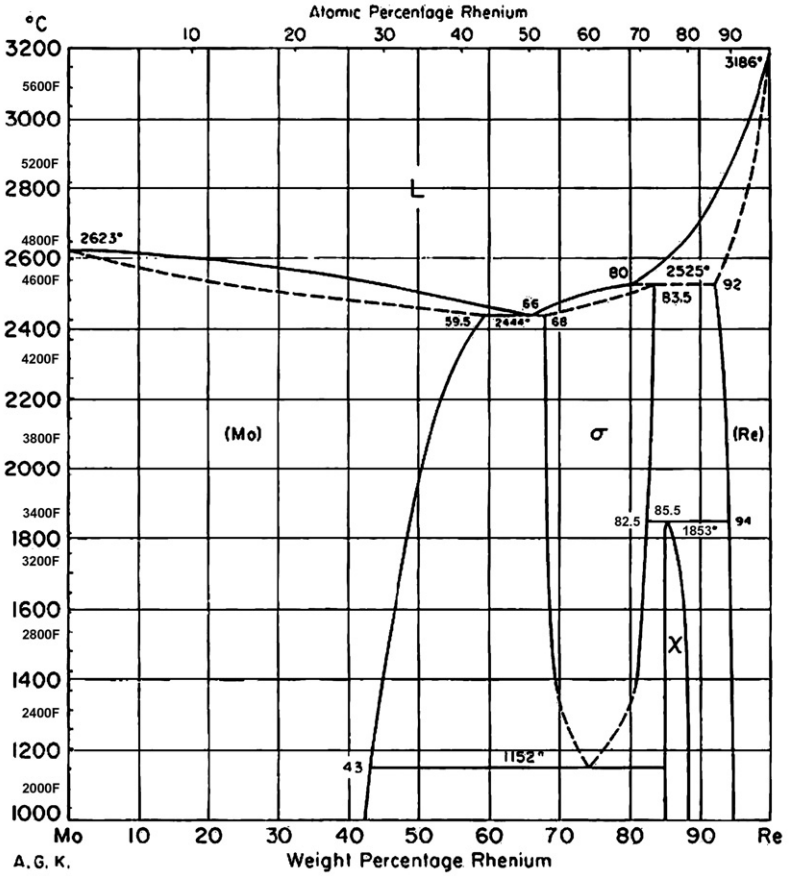

Fig. 1. Equilibrium phase diagram for the Mo–Re system (from Ref. [24]).

The works of Erck and Rehn, Hasegawa and Nemoto lead to the conclusion that Mo–Re alloys are susceptible to radiation-induced segregation and precipitation depending on several parameters, including composition, heat treatment, dose level, dose rate and irradiation temperature.

The issue of phase stability becomes even more important when the effects of transmutation are considered. Greenwood and Garner [25] have shown that Mo–Re alloys will transmute strongly to Mo–Re–Os–Ru–Tc alloys in a wide variety of neutron spectra, especially in highly thermalized spectra of light water reactors such as HFIR or SM-2. In a recent paper by Busby and coworkers, for example, a low dose of only 0.72 dpa in Mo–41–wt% Re irradiated in HFIR resulted in a transmuted composition of Mo–24Re–17Os [18].

As shown in Fig. 2(a) and (b), Greenwood and Garner also demonstrated that while fast reactor spectra in general led to much lower rates of transmutation, the spectral sensitivity of resonances in the epithermal range is strong enough that large differences in transmutation rates per dpa can occur between in-core and below-core regions of the FFTF reactor [25]. In a later experimental study by Garner and coworkers on pure Re irradiated in EBR-II and FFTF it was shown that relatively small spectral differences between in-core regions of the two fast reactors could significantly impact the interpretation of the data [26]. One consequence of increasing Os formation in Re is a reduced lattice parameter that induces significant and progressive densification of the evolving alloy.

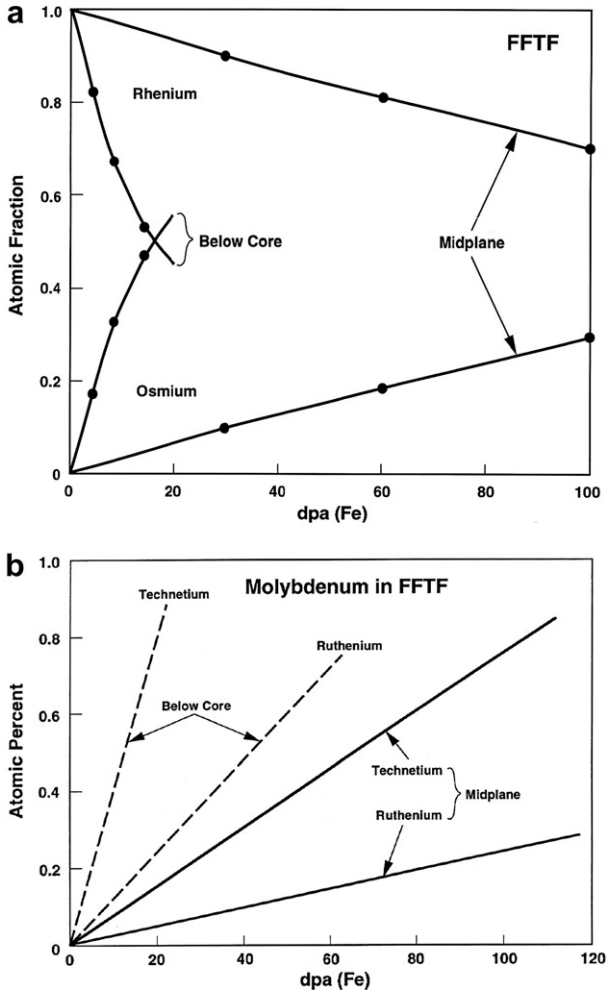

Fig. 2. Transmutation of (a) Re and (b) Mo in FFTF showing a strong sensitivity of transmutation to axial position in reactor. Note that doses were originally specified in terms of dpa for pure Fe, reflecting the large number of elements examined in Ref. [25]. In these FFTF studies Mo would experience only 87% of the dpa received by pure Fe.

These position-dependent differences in transmutation rate make it difficult to confidently combine and correlate data vs. dpa from different core locations without inadvertently conducting an unrecognized two-variable experiment. The chemical properties of Re and Os are sufficiently different that the progressive in-growth of Os probably will influence both the lattice parameter change and the phase stability of the evolving alloy.

In order to assess the combined impact of irradiation-induced segregation and transmutation on swelling, phase stability and microstructural evolution, pure Mo and Mo–41 wt% Re were irradiated side-by-side in FFTF. The density changes and microstructural results on pure Mo were published earlier [27]. Some of the microstructural results on Mo–41 wt% Re cited earlier was published earlier by Garner, Greenwood and Edwards [20], with the complete microstructural results presented in this paper.

2. Experimental details

Specimens of Mo–41Re (wt%) were irradiated in the form of standard 3mm diameter microscopy disks after preparation in two starting conditions. These conditions were: (a) annealed 1 h at 760 °C, followed by aging for two hours at 320 °C and (b) 20% cold-worked, and followed by aging for two hours at 320 °C.

The Mo–4Re and Mo specimens were enclosed in stainless steel 'weeper' packets which allowed contact with reactor sodium. At each irradiation temperature two identically-loaded packets were irradiated side-by-side in the fast flux test facility (FFTF), with one packet removed at the end of the first cycle and the other after the second cycle. Unirradiated archive material was available for comparison.

The temperatures in the materials open test assembly (MOTA) were actively controlled to remain within ±5 °C of the target level throughout the irradiation. As shown in Table 1 irradiation proceeded at target temperatures of 471, 569, 645, and 730 °C to two exposure levels, with dpa levels varying with target temperature. Two doses of 41 and 96 dpa were reached in capsules irradiated at 420 °C. In the latter stages of the 96 dpa irradiation at 420 °C, however, there was an over-temperature event followed by irregular and lower than target temperature sequences as described in reference [20]. Therefore less

Table 1
Density decreases (%) measured in Mo–41 wt% Re

Temperature (°C)	Fluence[a]	Fe (dpa)	Mo (dpa)	Annealed	Cold-worked
471	8.45	32.2	28	2.26	0.06
471	11.8	43.7	38	−0.28	−0.25
420	12.3	47.2	41	0.33	−0.08
420	27.6	110.8	96	0.11	0.28
569	10.6	40.8	35	0.72	1.14
569	16.9	65.8	57	0.82	0.12
645	10.6	40.8	35	0.66	0.043
645	16.9	65.8	57	1.41	0.15
730	10.6	40.8	35	1.45	0.47
730	15.9	61.5	53	0.07	−0.49

[a] Fluences quoted in units of 10^{22} n/cm^2 $E > 0.1$ MeV.

confidence is placed in data generated in the second segment of the irradiation conducted at 420 °C.

The dpa levels cited here were calculated for pure Mo calculated using the SPECTER code [28]. It is difficult to calculate more accurate dpa levels for Mo–Re and Mo–Re–Os alloys due to the lack of threshold energy data for Re and Os, and the dose/time dependence of the composition due to transmutation. Attempts to estimate the doses for the heavier Mo–41 Re alloy using Ta as a surrogate for Re, using a threshold displacement energy of 90 eV as recommended in ASTM E521, yields a reduction of ~28% from the dose experienced by pure molybdenum. This estimate ignores the progressively increasing contribution of Os with continued irradiation, however. Earlier studies by Hasegawa and Nemoto also faced the problem of how to calculate dpa for Mo–Re–Os alloys. They also chose to quote their dpa levels in terms of pure Mo and used the calculations cited in reference [28].

The initial and post-irradiation densities for all of the different conditions were determined by an immersion technique known to be accurate to 0.2% change in density. JEOL 1200EX and 2000ES transmission electron microscopes (TEM) were used in the analysis of the microstructure of selected specimens. Specimens for TEM were polished at room temperature and ~30 V using a 20% sulfuric and 80% ethanol electrolyte in a Tenupol electropolishing unit.

3. Results

Density decreases as large as 2% were observed after irradiation, varying with irradiation temperature, starting state of the alloy and dpa level. There is no easily discernible pattern to the density changes that develop in response to variations in temperature, starting state and dpa level.

As shown in Fig. 3 the density changes observed in four of the five irradiation sequences exhibited an 'overshoot' behavior for both starting conditions [20]. A similar behavior was also observed in pure Mo and was shown to be due to the competing kinetics of early void nucleation and the subsequent approach to a saturation

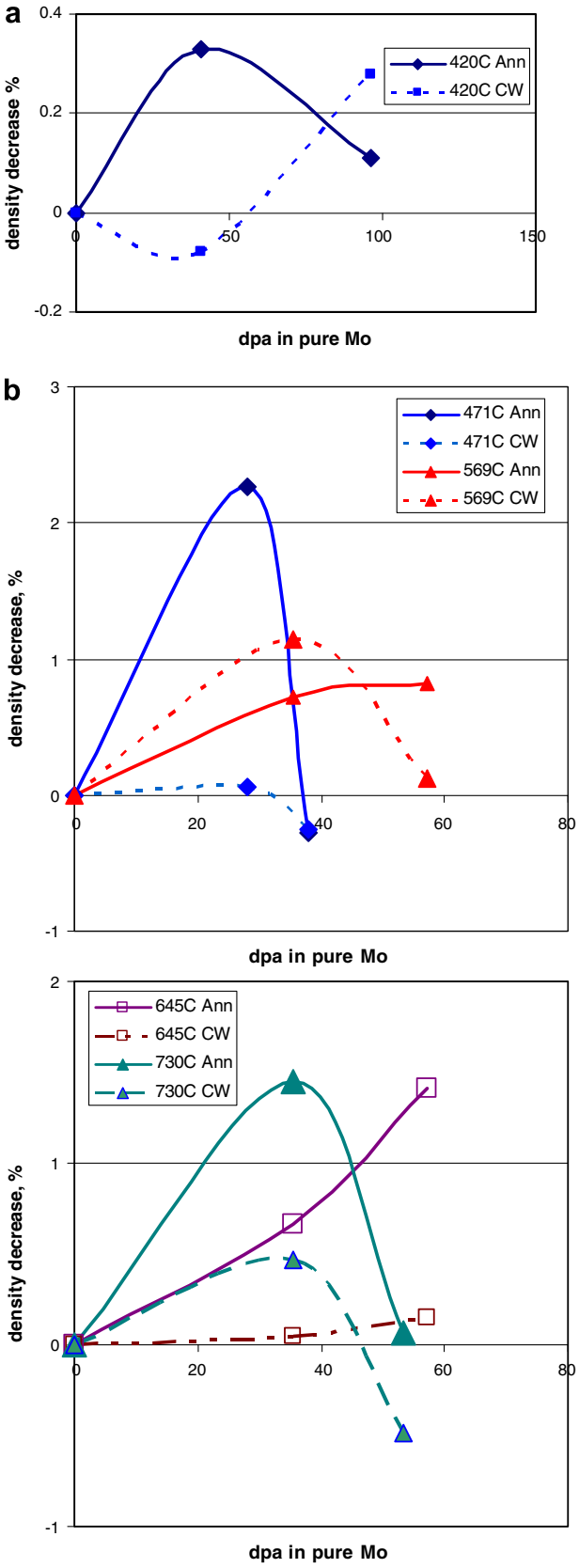

Fig. 3. Irradiation-induced density changes observed at (a) 420 °C and (b) 471–730 °C in Mo–41 wt% Re irradiated in FFTF (Ref. [20]). Ann refers to annealed and aged while CW refers to cold-worked and aged starting conditions.

state by void shrinkage associated with the development of a highly ordered void lattice [27]. Since the 'overshoot' behavior was observed in both pure Mo and Mo–41Re, there was initial speculation that a similar process involving void lattices might also have occurred in Mo–41 wt% Re. The expectation was found to be incorrect, however.

Electron microscopy of the unirradiated Mo–41Re specimens showed that both the cold-worked and aged and the annealed and aged specimens were single phase solid solutions of Mo and Re. This may indicate that the diffusion kinetics were too slow at the 320 °C ageing temperature to produce the equilibrium χ-phase (chi-phase) predicted in the phase diagram for the Mo–Re system (Fig. 1). In addition, the composition of Mo–41 wt% Re is such that very little of the chi-phase is predicted to be present according to the phase diagram. No significant dislocation density was observed in either the annealed and aged or the cold-worked and aged specimens. The lack of dislocations in the cold-worked and aged material suggests that the ageing treatment at 320 °C was sufficient to fully anneal the alloy. However, the lack of dislocations in either starting condition does not provide an explanation of why the radiation-induced density changes were different in the two starting conditions.

Due to the extensive precipitation that occurred during irradiation, selective electropolishing of the matrix appeared to have occurred in all specimens. This selective removal hindered the compositional analysis somewhat, especially that of the matrix.

Examination of the irradiated specimens revealed very few voids, certainly an insufficient number of voids to account for the observed decrease in density. Instead, for those specimens irradiated at temperatures of 420–730 °C, TEM analysis revealed a dense, complex microstructure with the dominant feature consisting of a high density of thin precipitate platelets in the interior of bcc Mo-rich grains. These precipitates overshadowed all other microstructural features such that no definitive measurements

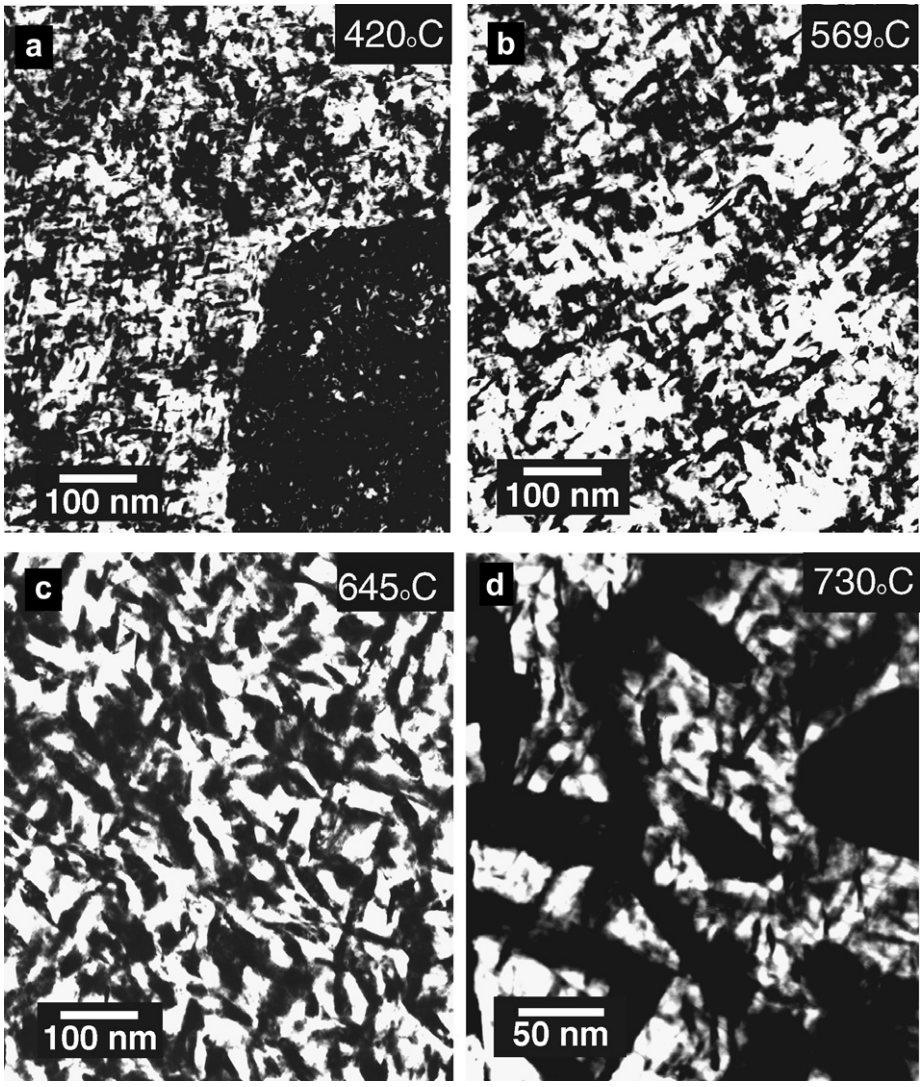

Fig. 4. Irradiation-induced precipitation observed at temperatures of (a) 420 °C at 96 dpa, (b) 569 °C at 57 dpa, (c) 645 °C at 57 dpa, and (d) 730 °C at 53 dpa in annealed and aged Mo–41 wt% Re.

could be of voids, dislocation loops or dislocation line segments.

Examples of the precipitate microstructure of the irradiated specimens are shown in Figs. 4–6 and 10, demonstrating qualitatively that the platelets increase in size as the irradiation temperature increases. Electron diffraction (Fig. 7) showed these precipitates to possess a hexagonal close-packed (hcp) crystal structure with lattice parameters of $a_0 = 0.284$ nm and $c_0 = 0.453$ nm, near that of pure Re within experimental error.

The diffraction pattern shown in Fig. 7(a) was taken ~7° off of the $\langle 1\,1\,1\rangle_{Mo}$ zone axis, demonstrating the orientation relationship derived for the hexagonal precipitates in the interiors of the grains as approximately:

$$\{0\,1\,1\}_{Mo} \| \{0\,0\,0\,1\}_{Re},$$
$$\langle 1\,1\,1\rangle_{Mo} \| \langle 2\,1\,1\,0\rangle_{Re}.$$

Subsequent tilting experiments confirmed the orientation relationship. In some cases, however, the precipitates were aligned such that the precipitate zone axis was superimposed on the matrix $\langle 1\,1\,1\rangle_{Mo}$ zone axis. The reason for this remains unclear, but it may be related to localized misorientation of the precipitates since the electropolishing tended to etch away the supporting Mo-rich matrix. The diffraction patterns shown in Fig. 7(b) and (c), respectively, were taken on the Mo $\langle 0\,1\,1\rangle$ and $\langle 0\,0\,1\rangle$ zone axes. The extra spots and streaks in the $\langle 0\,1\,1\rangle$ diffraction patterns could not be indexed, and are assumed to be a consequence of double diffraction and the thinness of the precipitate platelets.

In contrast to the results of Nemoto and coworkers no sigma phase precipitates were observed in Mo–41 wt% Re at any temperature or dose examined in this study. However, in the second irradiation segment at 730 °C and

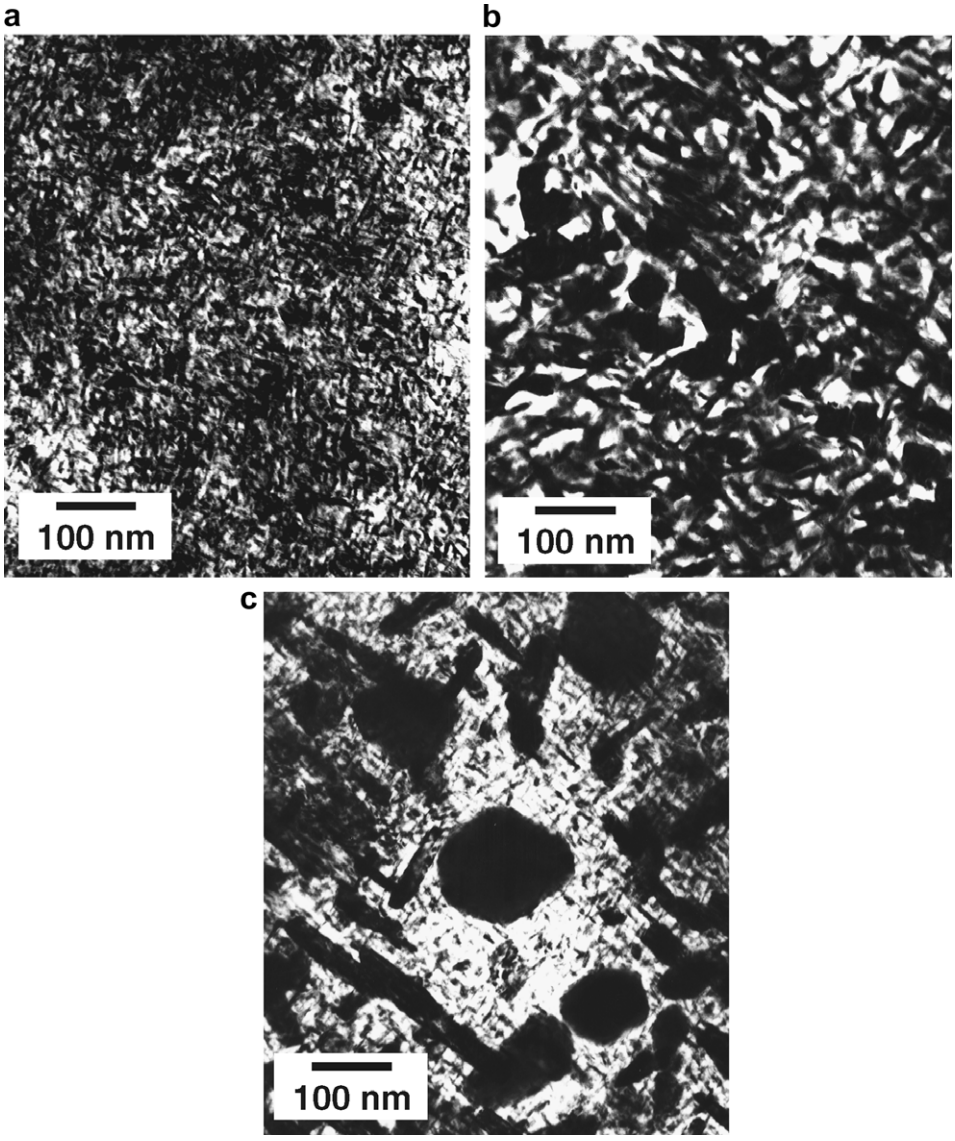

Fig. 5. Microstructures for the cold-worked and aged Mo–41 wt% Re irradiated at (a) 471 °C and 28 dpa, (b) 645 °C and 35 dpa, and (c) 730 °C and 35 dpa. Large chi-phase precipitates in (c) appear to be growing at the expense of the smaller hcp precipitates.

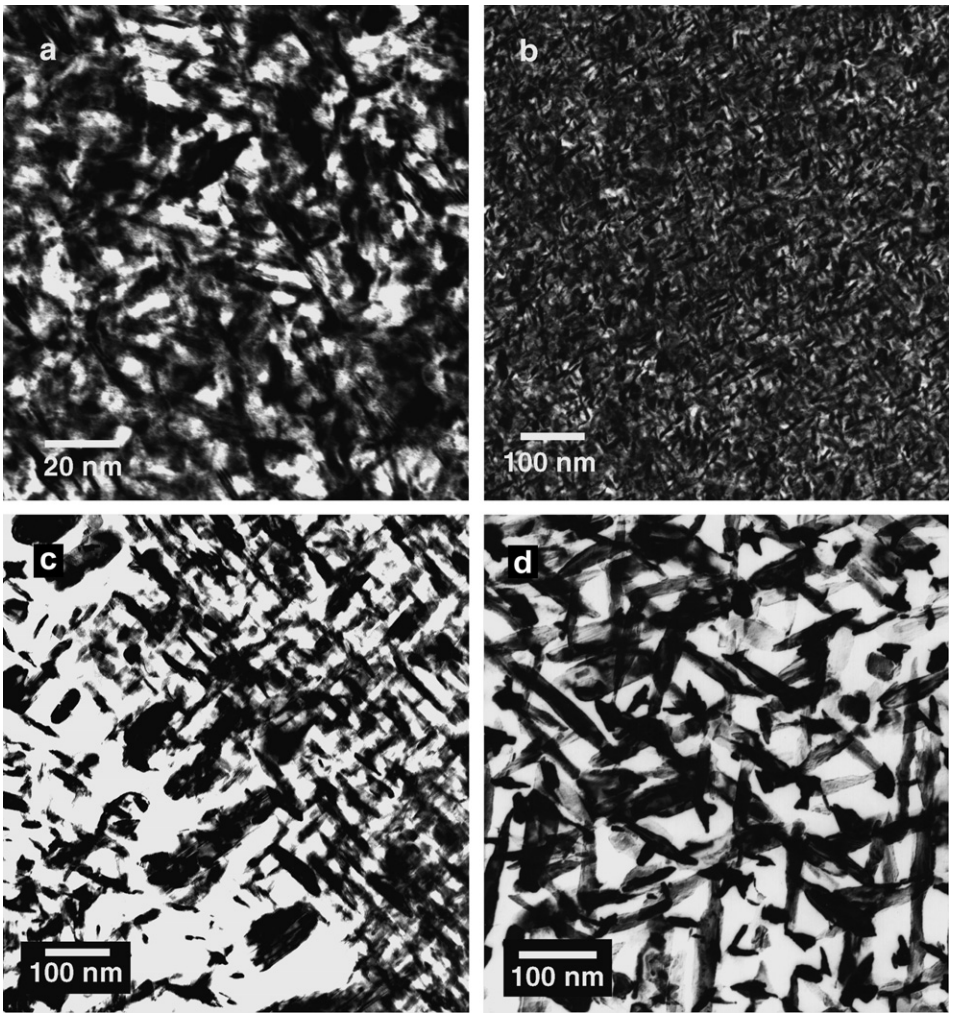

Fig. 6. Microstructures of Mo–41 wt% Re where (a) and (c) correspond to the cold-worked and aged specimens irradiated at 471 and 730 °C, respectively, while (b) and (d) correspond to the annealed and aged specimens irradiated at 471 and 730 °C, respectively. The dpa level at 427 °C is 28 dpa and is 35 dpa at 730 °C.

53 dpa an additional precipitate phase was occasionally found that possessed a much different appearance compared to the hcp phase. Examination of the specimens irradiated in the first irradiation segment to 35 dpa at 730 °C did not show any evidence of these precipitates, indicating that higher temperature, as well as higher dose and time at temperature are probably required to form this phase.

In Fig. 5(c) there are a number of these precipitates that are much larger and more equiaxed in appearance than the hexagonal phase. These particles were identified as bcc $MoRe_3$ (chi-phase) proposed by Knapton [29]. SAD patterns for the chi-phase are shown in Fig. 8, demonstrating that the precipitates possess a cube-on-cube orientation relationship with the molybdenum matrix, which agrees with the work of Erck and Rehn [21–23]. The lattice parameter was measured to be ~0.96 nm, almost identical to that measured separately by Knapton and by Erck and Rehn.

The hexagonal precipitates in the regions surrounding the large chi-phase precipitates at 53 dpa appear to be smaller in size, indicating that the hexagonal precipitates may be dissolving to form the chi-phase. A large number of the hcp phase precipitates still exist, however, and many of them have sizes approaching that of the chi-phase.

Selective electropolishing of the matrix made it relatively easy to obtain the composition of the precipitate phases but correspondingly harder to measure the composition of the matrix. The composition of the chi-phase precipitates at 730 °C to 53 dpa was measured to be approximately 45% Re, 15% Os, and 40% Mo by weight. EDS analysis of the hcp precipitates showed the composition at approximately 75% Re, 17% Os, and 8% Mo by weight in the same specimen. Typical examples of the EDS spectra from the two phases are given in Fig. 9.

The 8–9 wt% Mo measured in the hcp precipitates can not be confidently accepted and may reflect the inclusion of some matrix in the precipitate analysis. An accurate composition for the matrix could not be obtained because of the high density of precipitates and the lack of suitably large enough matrix volumes. Denuded zones were gener-

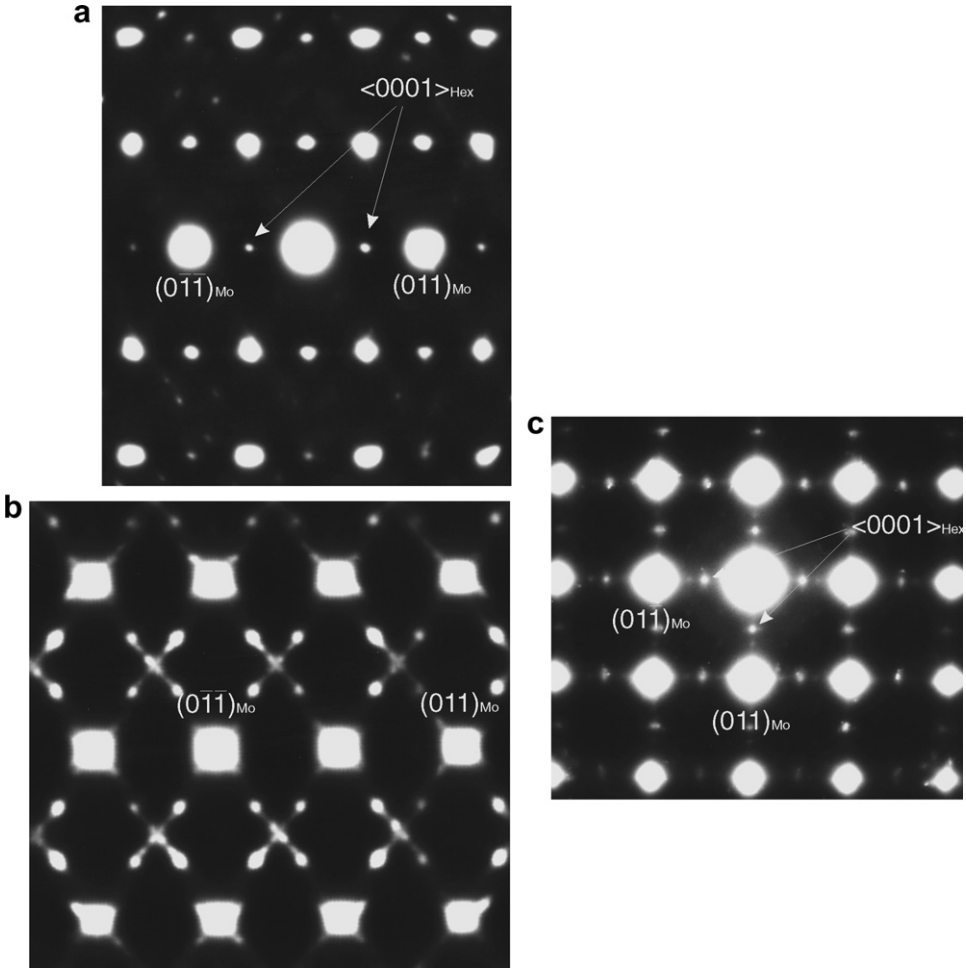

Fig. 7. Diffraction patterns from the hexagonal phase in the cold-worked and aged Mo–41 wt% Re irradiated at 730 °C and 35 dpa. The diffraction pattern in (a) was taken ~7°, off the ⟨1 1 1⟩ zone axis. The remaining two diffraction patterns (b) and (c) were taken exactly on the zone axes ⟨0 1 1⟩ and ⟨0 0 1⟩, respectively.

ally observed near grain boundaries and were the only regions free of precipitates. Although these regions were much higher in molybdenum, their compositions are not confidently thought to be representative of the matrix.

An additional difficulty encountered in determining the ratio of Re to Os involved overlap of peaks arising from the Re and Os, as shown in Fig. 9(a) and (b). However, the L_α peaks at 8.68 and 8.92 keV for Re and Os, respectively, were separated enough to allow an estimate to be made of the Os content.

Although Greenwood and Garner [25] predicted that Tc and Ru should be present at several tenths of a percent because of transmutation of the molybdenum, none of the EDS spectra contained peaks from either element detectable above the photon background arising from radioactivation. Taking spectra from thick regions, which included both the matrix and the precipitates, also did not yield any evidence of Tc and Ru. The peaks for the two elements should be easily separable at the higher energies if they are present in resolvable amounts. However, the selective electropolishing of the molybdenum matrix may have lowered the amount of Tc and Ru to levels below the detection limit. A similar observation concerning the absence of Tc and Ru signals was made by Hasegawa and coworkers on specimens irradiated in FFTF to 11–34 dpa [14].

As a general trend, it was observed that the lower the irradiation temperature, the smaller the size of the hcp precipitates and the higher their number density. The chi-phase precipitates tend to be larger and fewer in number in the cold-worked and aged specimens compared to the annealed and aged specimens.

Fig. 10 shows that the grain boundaries were sometimes found to be associated with extensive precipitation of a thick, equiaxed phase. Analysis of these grain boundary precipitates showed that they were also the Re-rich hcp phase.

4. Discussion

The Mo–Re equilibrium phase diagram predicts that at 400–700 °C Mo–41 wt% Re in the unirradiated condition should be comprised of a eutectoid mixture with a small fraction of chi-phase imbedded in a solid solution of bcc

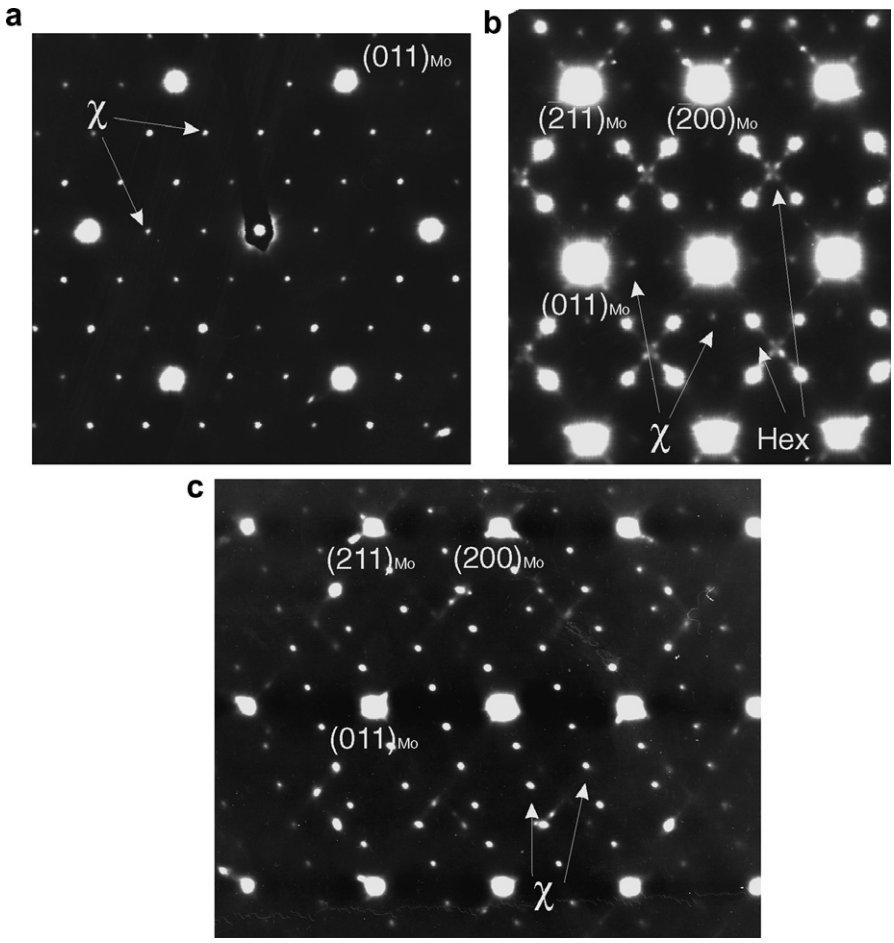

Fig. 8. Selected area diffraction patterns from the cubic chi-phase, demonstrating the cube-on-cube orientation relationship with the Mo matrix. The diffraction pattern in (a) is on the ⟨1 1 1⟩ zone axis, while (b) and (c) were both taken on the ⟨0 1 1⟩ zone axis. Note that (b) contains diffraction spots for both the hexagonal phase as well as the cubic chi-phase. The pattern in (c) shows one variant of the chi-phase precipitate.

Mo–Re. However, the TEM results show that the unirradiated Mo–41 wt% Re specimens were in fact single-phase. This failure to reach the anticipated equilibrium state is attributed to the rather low aging temperature and short aging time, as well as the close proximity to the phase boundary. Indeed, Leonard and coworkers showed that 1100 h aging of Mo–41 wt% Re in this temperature range resulted in no precipitation, while similar aging of Mo–47.5 wt% Re resulted in both sigma-phase and chi-phase precipitation [5].

In the irradiated Mo–41 wt% Re specimens of the current study, however, it was observed that the non-equilibrium hexagonal closed-packed phase was very easily formed at all conditions examined. This reflects a tendency toward radiation-induced segregation of Re so strong as to produce a phase that should exist only on the far right of the Mo–Re phase diagram. The segregation is so strong as to also bypass the formation of the slower-forming equilibrium chi-phase.

The observation that the equilibrium chi-phase can also form at 730 °C after sufficiently high dose and time agrees qualitatively with Erck and Rehn's observation that chi-phase only formed in their ion-irradiated specimens when the irradiation temperature was 750 °C or higher.

Erck and Rehn [21–23] have studied the segregation of Re to the front surface of ion-bombarded Mo–xRe alloys, where $x = 13$, 42, and 45 wt%. The ion irradiation was conducted over the temperature range of 550–1255 °C. Their study was conducted at a higher displacement rate compared to that of neutron irradiation and did not involve transmutation. In addition, they were limited to doses of ~1 dpa due to blistering of the surface from the ion-implanted He atoms. They found that chi-phase formation only occurred in Mo–Re alloys with 42 and 45 wt% Re, and then only in the temperature range (750–1075 °C) where enough segregation occurred that the Re concentration near the foil surface exceeded the solid solubility of Re in Mo (~42 wt% Re). Irradiation of the Mo–13 wt% Re alloy produced Re levels of ~14 wt% Re in the near-surface regions of the foils, far below the solid solubility limit, and consequently no chi-phase was formed.

Erck and Rehn modeled the segregation in terms of preferential segregation of the heavier but 'undersized' Re atoms (based on King's work on size factors [30])

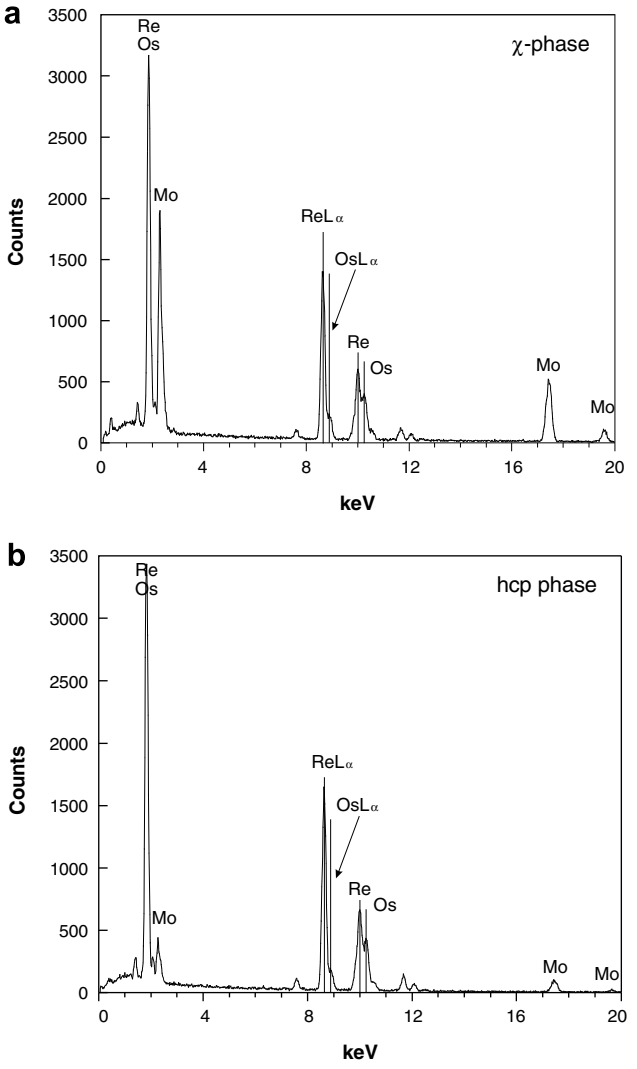

Fig. 9. EDS measurements of (a) a hexagonal precipitate and (b) chi-phase precipitate in the Mo–41 wt% Re irradiated at 730 °C and 35 dpa.

by an interstitial mechanism. King reported in his tabulation of size factors that Re has a volume size factor 5.56% less than that of Mo, and a linear size factor 1.89% less than Mo. However, these values are for a maximum concentration of 15 wt% Re in solid solution, so their applicability to Mo–41Re is suspect since this exceeds the solubility of Re at temperatures less than 650 °C. There was no corresponding data listed for Re with Mo added as solute.

The impact of the Os on precipitation is not known, however. Although Re and Os exhibit complete solid solubility in each other, they do have much different volume size factors in Mo (−9.62% for Os vs. −5.56% for Re). Based on the size factors alone, both Re and Os should segregate toward boundaries in Mo, though most likely at different rates. Additionally, the progressive transmutation of Re to Os should eventually lead to an increase in density with time, as was indeed observed in most specimens.

Nemoto and coworkers [17] noted that the ratio of Re/Os in the 'sigma' phase in Mo–10 wt% Re was very similar to that of the matrix in irradiated Mo–Re alloys, 0.25 vs. 0.22, respectively, at ~20 dpa, implying that the precipitates formed early and the majority of the transmutation occurred afterwards. In our study of Mo–41 wt% Re the ratios for the hcp and chi phases were 0.23 at ~40 dpa and 0.33 at 53 dpa, respectively.

The authors of the current study are not convinced that Nemoto observed sigma phase at all Re levels, especially at 41 wt% Re. Nemoto drew on his parallels with his more-detailed work on W–Re alloys to identify the phases in Mo–Re alloys. He may have correctly identified sigma-phase in the 2–13 wt% Re range, but it is not clear from his paper that sufficient attention was directed toward the Mo–41 wt% Re alloy, whereas our study showed that the hcp Re-rich phase forms easily at all temperatures examined.

In comparison to the work of Erck and Rehn where only chi-phase was observed at 41 wt% Re, our work indicates that the formation of the hcp precipitates during neutron irradiation is much more dominant. This difference may be related either to the lower displacement rate inherent in neutron irradiation and/or to the formation and participation of osmium in the precipitation process. Osmium may have segregated concurrently with rhenium, but probably also formed by transmutation in the Re precipitates after they formed. However, the morphology and size of the hcp precipitates suggests that the precipitates arise primarily and very quickly due to very strong radiation-induced segregation to radiation-induced interstitial loops.

The initial density decreases or 'apparent swelling' observed in Mo−41 wt% Re in this experiment did not arise as a consequence of void formation as was originally anticipated. Therefore, it must have arisen from formation of the non-equilibrium hcp phase and the removal of Re from solution. Since Mo–41 wt% Re has a density 134% that of pure Mo (10.22 g/cm^3) according to our experimental measurements, and pure Re and Os both have densities of around 20 g/cm^3, segregation of Re could easily produce overall volumetric dilations as large as several percent. Subsequent formation of Os would tend to densify the alloy and most likely accounts for the non-monotonic behavior of the density with dose.

The observed radiation-induced microstructural changes in this study are so overwhelming that they may preclude the application of Mo–Re alloys with high Re (>40%) content as structural materials in neutron environments, at least in the temperature range (430–730 °C) of the current study. While Busby and coworkers [18] showed that tensile tests on Mo–41Re did not exhibit brittle failure when the alloy was irradiated above 800 °C to ~1 dpa in HFIR, Hasegawa and coworkers demonstrated very brittle behavior after irradiation at 373–800 °C in FFTF to doses comparable (7–34 dpa) to those of the current study [16,17]. While the doses attained in the two cited studies are quite different, the transmutation levels in the specimens of Busby and Hasegawa are more comparable. It is

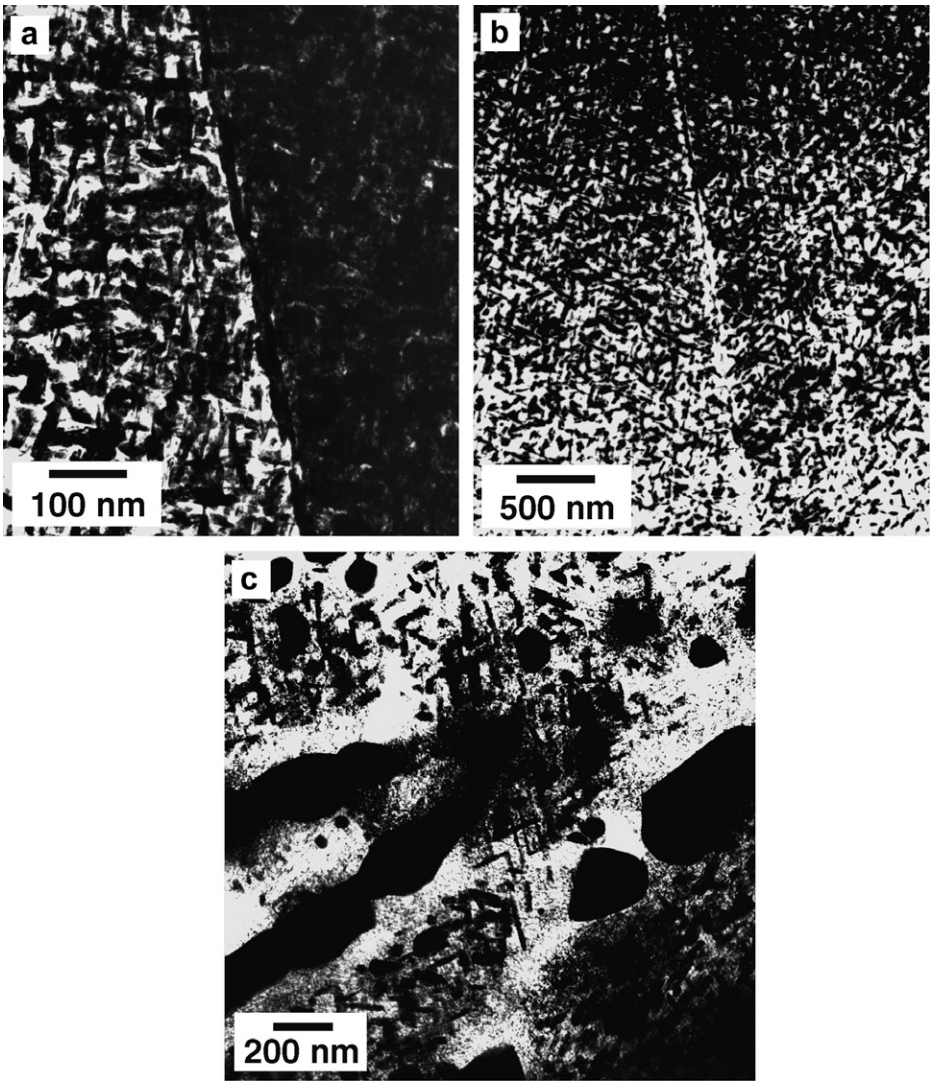

Fig. 10. Examples of the grain boundary hcp precipitates in specimens irradiated under at (a) 645 °C, 35 dpa, annealed and aged, (b) 730 °C, 35 dpa, annealed and aged, and (c) 730 °C and 53 dpa, cold-worked and aged. Large grain boundary hcp precipitates in (c) appear to be growing at the expense of the smaller hcp precipitates.

reasonable to wonder, however, if Busby's results would shift toward a more brittle behavior of Mo–41Re if the dpa levels were closer to the levels obtained in FFTF. Indeed Busby saw a drop in ductility in Mo–47.5Re relative to that of Mo–41Re in the same experiment, suggesting that a larger chemical driving force and perhaps a longer exposure might produce less ductility in Mo–41Re than observed in his relatively low dose study.

5. Conclusions

The combined influence of both strong neutron-induced segregation and transmutation of Re in Mo–41 wt% Re has strong consequences on its phase stability. Radiation in the range 420–730 °C induced complete instability of the alloy matrix involving the formation of a non-equilibrium Re-rich phase to form in lieu of the anticipated chi-phase. Only at the highest temperature and highest dose explored was the equilibrium chi-phase observed to form and compete with the hcp phase. The observed microstructural changes are so pronounced that they may preclude the application of Mo–Re alloys with high Re content as structural materials in neutron environments.

Acknowledgements

This work was performed under the sponsorship of the US Department of Energy, Office of Fusion Energy Sciences under contract DE-AC06-76RLO 1830. Battelle Memorial Institute operates Pacific Northwest National Laboratory for U.S.D.O.E.

References

[1] G.M. Kalinin, J. Nucl. Mater. 179–181 (1991) 1193.
[2] V.V. Rybin, D.L. Smith, J. Nucl. Mater. 191–194 (1992) 30.

[3] F.W. Wiffen, in: R.J. Arsenault (Ed.), Defects and Defect Clusters in BCC Metals and Their Alloys, National Bureau of Standards, Gaithersburg, MD, 1973, p. 176.
[4] Y. Hiraoka, M. Okada, H. Irie, J. Nucl. Mater. 155–157 (1988) 381.
[5] K.J. Leonard, J.T. Busby, S.J. Zinkle, J. Nucl. Mater. 366 (2007) 336, and also 369.
[6] I.V. Gorynin, V.A. Iganotov, V.V. Rybin, S.A. Fabritsiev, V.A. Kazakov, V.P. Chakin, V.A. Tsykanov, V.R. Barabash, Y.G. Prokofyev, J. Nucl. Mater. 191–194 (1992) 421.
[7] S.A. Fabritsiev, V.A. Gosudarenkova, V.A. Potapova, V.V. Rybin, L.S. Kosachev, V.P. Chakin, A.S. Pokrovsky, V.R. Barabash, J. Nucl. Mater. 191–194 (1992) 426.
[8] T. Tanabe, N. Noda, H. Nakamura, J. Nucl. Mater. 196–198 (1992) 11.
[9] G. Filacchioni, E. Casagrande, U. DeAngelis, G. DeSantis, D. Ferrara, J. Nucl. Mater. 212–215 (1994) 1288.
[10] G.V. Mueller, D. Gavillet, M. Victoria, J.L. Martin, J. Nucl. Mater. 212–215 (1994) 1283.
[11] B.N. Singh, A. Horsewell, P. Toft, J.H. Evans, J. Nucl. Mater. 212–215 (1994) 1292.
[12] B.N. Singh, J.H. Evans, A. Horsewell, P. Toft, D.J. Edwards, J. Nucl. Mater. 223 (1995) 95.
[13] V.P. Chakin, F. Morito, V.A. Kazakov, Yu.D. Goncharenko, Z.E. Ostrovsky, J. Nucl. Mater. 258–263 (1998) 883.
[14] A. Hasegawa, K. Abe, M. Satou, C. Namba, J. Nucl. Mater. 225 (1995) 259.
[15] S.A. Fabritsiev, A.S. Pokrovsky, J. Nucl. Mater. 252 (1998) 216.
[16] A. Hasegawa, K. Ueda, M. Satou, K. Abe, J. Nucl. Mater. 258–263 (1998) 902.
[17] Y. Nemoto, A. Hasegawa, M. Satou, K. Abe, Y. Hiraoka, J. Nucl. Mater. 324 (2004) 62.
[18] J.T. Busby, K.J. Leonard, S.J. Zinkle, J. Nucl. Mater. 366 (2007) 388.
[19] Y. Nemoto, A. Hasegawa, M. Satou, K. Abe, J. Nucl. Mater. 283–287 (2000) 1144.
[20] F.A. Garner, L.R. Greenwood, D.J. Edwards, J. Nucl. Mater. 212–215 (1994) 426.
[21] R.A. Erck, L.E. Rehn, J. Nucl. Mater. 208–219 (1989) 168.
[22] R.A. Erck, L.E. Rehn, Philos. Mag. A 29–51 (1990) 62.
[23] R.A. Erck, C.M. Wayman, L.E. Rehn, in: F.A. Garner, N.H. Packan, A.S. Kumar (Eds.), Radiation-induced Changes in Microstructure: 18th International Symosium (Part 1), ASTM STP 955, American Society for Testing and Materials, Philadelphia, 1987, p. 721.
[24] T.B. Massalski, H. Okamoto (Eds.), Binary Alloy Phase Diagrams, 2nd Ed., ASM International, Metals Park, OH, 1990, p. 2656.
[25] L.R. Greenwood, F.A. Garner, J. Nucl. Mater. 212–215 (1994) 635.
[26] F.A. Garner, M.B. Toloczko, L.R. Greenwood, C.R. Eiholzer, M.M. Paxton, R.J. Puigh, J. Nucl. Mater. 283–287 (2000) 380.
[27] F.A. Garner, J.F. Stubbins, J. Nucl. Mater. 212–215 (1994) 1298.
[28] F.A. Garner, L.R. Greenwood, A.M. Ermi, in: Fusion Reactor Materials Semiannual Progress Report for Period Ending March 31, 1992, DOE/E-0313/12, p. 54.
[29] A.G. Knapton, J. Inst. Met. 87 (1959) 62.
[30] H.W. King, J. Mater. Sci. 1 (1966) 79.